



A synchrotron beamline for extreme-ultraviolet photoresist testing

C. Tarrio, S. Grantham, S. B. Hill, N. S. Faradzhev, L. J. Richter, C. S. Knurek, and T. B. Lucatorto

Citation: *Review of Scientific Instruments* **82**, 073102 (2011); doi: 10.1063/1.3606484

View online: <http://dx.doi.org/10.1063/1.3606484>

View Table of Contents: <http://scitation.aip.org/content/aip/journal/rsi/82/7?ver=pdfcov>

Published by the AIP Publishing

Articles you may be interested in

Actinic critical dimension measurement of contaminated extreme ultraviolet mask using coherent scattering microscopy

J. Vac. Sci. Technol. B **32**, 031601 (2014); 10.1116/1.4873697

Carbon contamination and oxidation of Au surfaces under extreme ultraviolet radiation: An x-ray photoelectron spectroscopy study

J. Vac. Sci. Technol. B **30**, 041603 (2012); 10.1116/1.4737160

Synchrotron beamline for extreme-ultraviolet multilayer mirror endurance testing

Rev. Sci. Instrum. **76**, 056101 (2005); 10.1063/1.1896225

Outgassing of photoresists in extreme ultraviolet lithography

J. Vac. Sci. Technol. B **18**, 3402 (2000); 10.1116/1.1321754

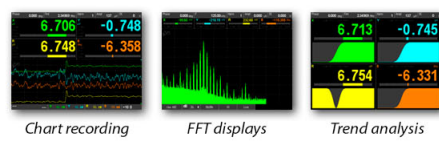
Outgassing of photoresist materials at extreme ultraviolet wavelengths

J. Vac. Sci. Technol. B **18**, 3364 (2000); 10.1116/1.1314383

The new SR865 **2 MHz Lock-In Amplifier ... \$7950**



 **Stanford Research Systems**
www.thinkSRS.com · Tel: (408)744-9040



Features

- Intuitive front-panel operation
- Touchscreen data display
- Save data & screen shots to USB flash drive
- Embedded web server and iOS app
- Synch multiple SR865s via 10 MHz timebase I/O
- View results on a TV or monitor (HDMI output)

Specs

- 1 mHz to 2 MHz
- 2.5 nV/√Hz input noise
- 1 μs to 30 ks time constants
- 1.25 MHz data streaming rate
- Sine out with DC offset
- GPIB, RS-232, Ethernet & USB

A synchrotron beamline for extreme-ultraviolet photoresist testing

C. Tarrio,^{a)} S. Grantham, S. B. Hill, N. S. Faradzhev, L. J. Richter, C. S. Knurek, and T. B. Lucatorto

National Institute of Standards and Technology, Gaithersburg, Maryland 20899, USA

(Received 4 May 2011; accepted 8 June 2011; published online 11 July 2011)

Before being used in an extreme-ultraviolet (EUV) scanner, photoresists must first be evaluated for sensitivity and tested to ensure that they will not contaminate the scanner optics. The new NIST facility described here provides data on the contamination potential of the outgas products of a candidate resist by simultaneously irradiating a multilayer optic and a nearby resist-coated wafer with EUV radiation. The facility can also be used without changing its configuration to provide accurate resist dose-to-clear measurements. Detailed, real-time information on the rate of contamination growth is given by a unique, *in situ* imaging ellipsometer. We will describe the optical layout, mechanical design, and capabilities of the beamline, finally presenting experimental examples of its capabilities.

[doi:10.1063/1.3606484]

I. INTRODUCTION

Extreme ultraviolet lithography (EUVL; Ref. 1) is likely to displace current 193 nm optical lithography to produce semiconductor circuits beyond the 22 nm generation. This technology uses light with a wavelength of 13.5 nm and near-normal-incidence reflective Mo-Si multilayer mirrors to demagnify and image features from a reflective mask patterned with an absorber. The mirrors are protected against possible oxidation due to residual water vapor in the unbaked vacuum environment by a passivating cap layer, typically Ru or TiO₂ [Ref. 2]. Although these cap layers reduce the risk of oxidation of the multilayer structure, they do not prevent carbon deposition from low levels of residual organic molecules that can be cracked by the high-intensity EUV radiation. The latter is thus the primary source of optics degradation. To minimize this risk, EUVL scanners are constructed entirely of ultrahigh-vacuum-compatible materials. The outgassing of contaminating organic species during EUV exposure of the resist, however, is unavoidable. Various vacuum design strategies are employed to minimize transmission of these vapors to the optics, but the primary defense is to identify and avoid resists with the greatest potential for optics contamination.³

To be inserted into an advanced scanner, resists must first be qualified to ensure that they will not excessively contaminate the optics or produce an irreversible degradation. Several attempts to evaluate resists indirectly have been made, for example, by performing a chemical analysis of the outgas products⁴ and then subsequently studying the EUV-induced contamination of sample optics caused by the identified individual components or related molecular systems.⁵ However, due to the large number of potentially relevant species and the complex pressure and intensity scaling of the individual contamination rates observed to date, this strategy has not provided a robust measure of the actual damage potential a given resist may pose to the optics under realistic operating conditions. Hence, a more straightforward method to provide

a test that simulates conditions in an actual stepper has been introduced for qualifying resists.⁶ This so-called witness sample test involves simultaneous EUV irradiation of a 13.5 nm multilayer mirror sample and a photoresist-coated wafer. The thickness of the resulting (mostly carbon) contamination of the witness sample is then determined along with how well it can be removed from the sample with a cleaning technique that does not affect the surface of the optic, with the thickness and post-cleaning residue criteria set by the tool manufacturer.

While this witness sample test using EUV radiation is expected to be a good predictor of performance in an actual scanner, the limited availability of EUV sources capable of providing sufficiently high intensity for such tests has motivated the effort in the industry to establish an equivalency between witness plate tests performed with EUV photons and with electrons. Past observations have shown that such equivalences can be established as is to be expected since both EUV irradiation and e-beam irradiation produce secondary electrons which are thought to be major participants in the surface reactions of adsorbed molecules.⁷ Before this equivalence can be established, a broad base of knowledge derived from EUV-based exposures is necessary. The National Institute of Standards and Technologies (NIST) Synchrotron Ultraviolet Radiation Facility (SURF III; Ref. 8) is a metrology-dedicated storage ring with a peak output near 13.5 nm making it near ideal for performing the witness sample test with EUV radiation as originally specified. We have recently designed and installed a new branch on an existing beamline that allows witness sample testing of resists with fairly rapid turnaround. We will present the design of the optical system, sample chamber, and *in situ* diagnostics. We will also present the performance of the beamline in terms of throughput, wafer exposure, and post-exposure metrology.

II. FACILITY DESIGN

In order to serve as a good proxy for the conditions expected in a scanner, the NIST beamline had to meet the following several criteria as described in Ref. 6:

^{a)}Author to whom correspondence should be addressed. Electronic mail: charles.tarrio@nist.gov.

- (1) Sufficient EUV intensity at the witness sample so that the photo-induced carbonization rate is independent of intensity (i.e., the rate is intensity-saturated).
- (2) A maximum distance of 20 cm between illuminated wafer and the witness sample.
- (3) A resist dose with in-band 13.5 nm radiation that is uniform over an entire 200 mm wafer.
- (4) A chamber base pressure is in the low 10^{-9} mbar region with maximum pumping speed of 200 l/s to provide adequate partial pressure of outgas products with minimal interference from background gases.

The first criterion ensures that every molecule that sticks to an optical surface will react with a photon, either by cracking or undergoing photon-stimulated desorption, as is known to happen in the tool. This factor removes the requirement for precise intensity stability within a given testing facility or tight comparability of intensities between different facilities as a concern when evaluating results. The second criterion provides an amount of accelerated testing in that choosing a distance to be less than 20 cm (along with a pumping speed less than 200 l/s) creates conditions in which a measurable amount of contamination will occur with the exposure of a single 200 mm wafer. The third requirement is important in order to ensure that the same amount of resist outgas is being tested from run to run and from laboratory to laboratory. The uniform dose is set at E_0 since at much beyond a clearing dose there is the possibility that the outgas components may change significantly. Finally, the pumping speed limit ensures that adequate partial pressures of outgas components are present near the sample to accelerate the test and the upper limit on background gases, especially species such as water vapor that can considerably mitigate carbon deposition, reduces the possibility of spurious effects that will distort the results.

The optical layout of our beamline is shown in Fig. 1. Even though the broadband power of SURF III output near 13.5 nm is many times greater than that from a typical laboratory source, the amount of power in the narrow spectral band that is reflected by a multilayer mirror tuned to 13.5 nm is not enough to simultaneously ensure intensity saturation on the witness sample and a reasonable exposure time for the wafer. Since the wavelength of the irradiation is expected to have minimal effect on the amount of contamination when operating in an intensity-saturated mode, we decided to irradiate the witness sample with the higher power of the broadband radiation collected from 20 mrad of the horizontal emittance and the entire vertical emittance of SURF III using a rhodium-

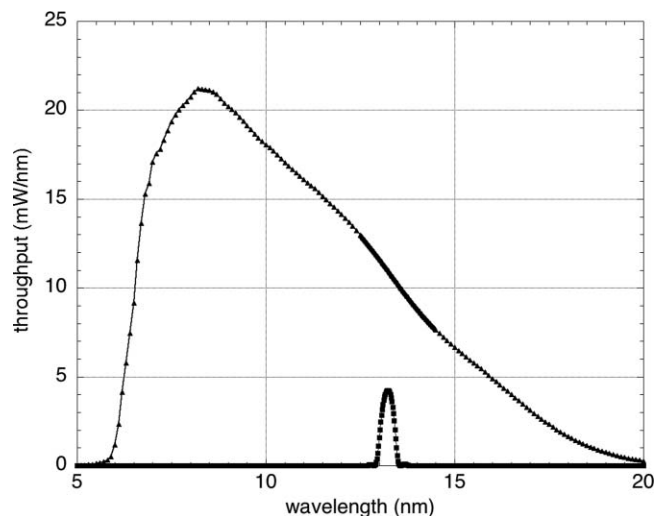


FIG. 2. Spectral power estimated from component measurements and calculated SURF output. Triangles: spectral power incident on the multilayer witness sample. Squares: spectral power incident on the wafer after two multilayer reflections.

coated toroidal mirror with a 10° grazing angle of incidence. The radiation is further filtered by a $0.25 \mu\text{m}$ thick Zr foil captured in the gate of a gate valve, which also serves as a low-pressure vacuum seal to prevent upstreaming of contaminants from the photoresist. The spectral power transmitted by the mirror-filter combination is shown in Fig. 2.

The toroidal collecting mirror has a sagittal radius of 9.98 m and a meridional radius of 0.30 m. With a 10° angle of incidence and source distance of 260 cm, we obtain an image at 130 cm with magnification of 0.5. Fine adjustment of the mirror position and angle are achieved through an external six-strut mount that provides six-axis alignment of the entire chamber.⁹ The full width at half maximum of the focused Gaussian beam on the witness sample obtained from ray tracing is 2.5 mm horizontal by 1.08 mm vertical with an assumed synchrotron beam size of 4.5 mm by 2.0 mm. We have experimentally characterized the beam spot by placing a thin scintillator crystal in the sample plane. The observed intensity distribution is approximately Gaussian with a small amount of coma, which is most likely due to yaw misalignment in the collecting mirror. Under beam conditions that were nominally those assumed in the ray tracing calculations, we measure a beam size of 2.2 mm by 1.04 mm. These values are within the $\sim \pm 10\%$ uncertainty of the ray tracing calculation and similar experimental uncertainty due to uncertainties in the measurement of distances, in the alignment of the mirror, and in the determination of the magnification of the imaging system.

As seen in Fig. 3, the 13.5 nm light reflected from the multilayer witness sample impinges on a fold mirror (also a multilayer mirror tuned to 13.5 nm) that reflects the radiation back parallel to its original path. Finally the radiation, at this point a spectrally narrow band centered at 13.5 nm by the two reflections, is incident on the 200 mm resist-coated wafer. Ray tracing and static photoresist exposures indicate that an arc of radiation of about 2 mm by 5 mm is incident on the wafer. This large size is due to the large divergence of roughly 5 mrad vertical by 20 mrad horizontal.

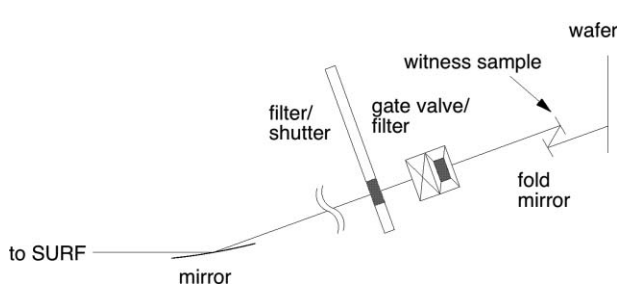


FIG. 1. Optical layout of EUV witness-sample testing beamline.

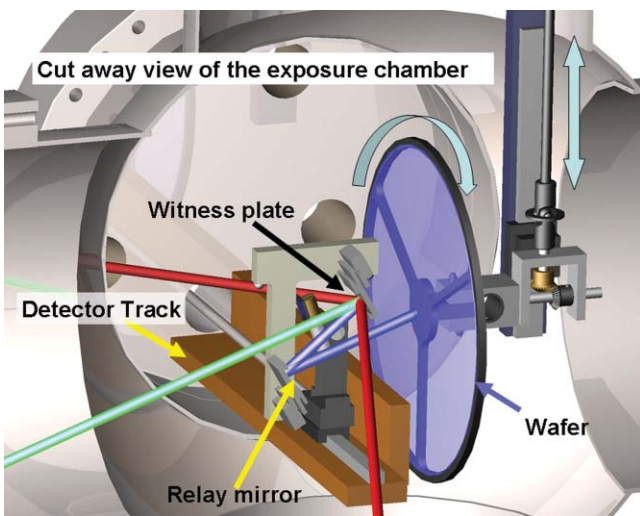


FIG. 3. (Color) Schematic of sample chamber and beamline. The red beam is the 635 nm beam of the NEIS laser; the green beam is the broadband (5 nm–20 nm) radiation incident on the witness sample; the blue beams are the narrowband (13.5 nm) radiation resulting from the reflections from the multilayer surfaces.

The uniform exposure of the entire wafer is accomplished by programmed coordination between the storage ring beam current, the rotation speed of the wafer and its linear scan rate across the incident EUV beam. A bellows-sealed rotary feedthrough rotates the wafer through a 90° gear box. To avoid any sulfur- or hydrocarbon-containing lubricants, we have replaced the stainless-steel bevel gears with PEEK (a low-outgassing polymer) and the stainless-steel rotary ball bearings with ceramic bearings. The rotation rate of the wafer along with the relatively slow translation are computer-controlled to over-write each point on the wafer five times within the beam image to ensure uniform dosing.

III. METROLOGY

A. Radiometry of EUV exposures

As mentioned earlier, the spectral distribution of the radiation incident on the witness sample was derived by multiplying the spectral power density of the SURF output with the measured reflectivity of the Rh-coated grazing incidence collection mirror and the measured transmission of the Zr filter. Similarly, the spectral distribution of the radiation incident on the resist was obtained by multiplying the incident radiation by the reflectances of the witness sample and the fold mirror. (see Fig. 2.) Two NIST-calibrated EUV-sensitive photodiodes¹⁰ are used in the sample chamber, one to measure the power incident on the witness sample and the other to measure the power incident on the photoresist-coated wafer. To reduce the power incident on the incident-radiation diode in order to avoid saturation, a Zr attenuating filter of about 0.7 μm thickness is incorporated into its mount. The attenuating filter is not used to measure the power on the wafer, since the reduced power after two reflections provides sufficient attenuation. The transmittance of the filter integrated over the bandwidth of the beamline was measured to be $4.8\% \pm 0.5\%$. The power incident on the witness sample is about 165 mW

at a typical operating beam current of 250 mA, while that incident on the resist-coated wafer is about 1.2 mW.

B. Real-time measurement of contamination rate

As mentioned, the facility provides for the simultaneous EUV exposure of a resist and a witness sample in a configuration that is meant to simulate the conditions in a real stepper. Following EUV exposures, the contamination on the witness sample must be analyzed to determine whether or not it exceeds certain limits as defined by the toolmaker. The analysis will include a measure of the thickness of the contamination and of the cleanability, which includes a determination of the molecular and elemental nature of the post-cleaning residue.

The predominant contamination to be expected is carbon. To monitor the rate of growth of carbon thickness

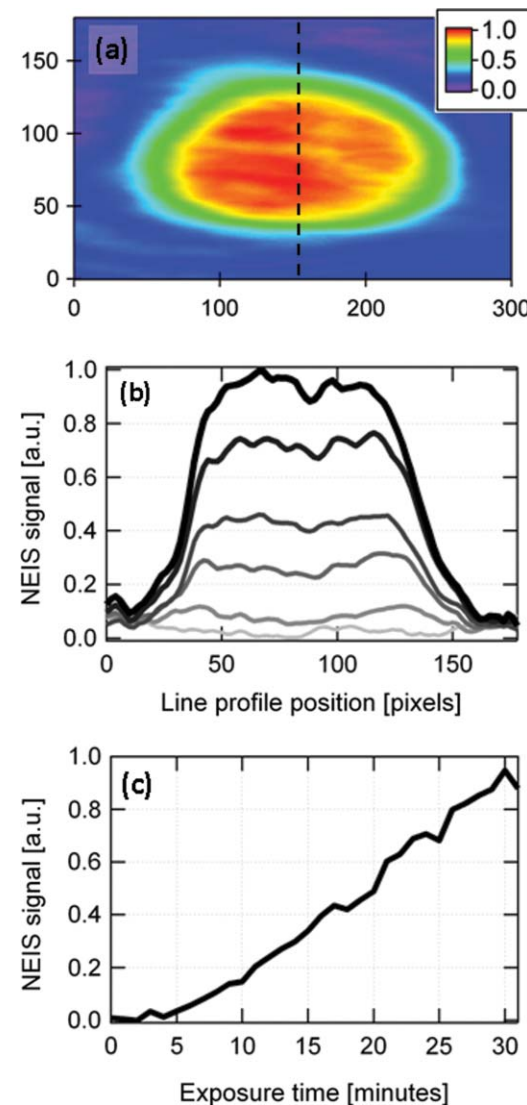


FIG. 4. (Color) (a) Normalized NEIS image of contamination formed on witness plate after 30 min of EUV exposure to resist outgassing. NEIS signal is equal to square root of CCD intensity, which is approximately proportional to thickness for thin C deposits. Values plotted here have been normalized to maximum NEIS amplitude at end of exposure. (b) Normalized NEIS signal along line shown in (a) at 6 min time intervals during exposure. (c) Evolution of normalized NEIS signal at center of exposure spot as function of time during exposure.

in situ during the exposure, we have designed and installed a null-field ellipsometric imaging system (NEIS).¹¹ It consists of the collimated output of a 635-nm diode laser that passes through a polarizer and compensator (quarter-wave plate) before reflecting from the sample at 70° angle of incidence to another polarizer placed in front of a high-spatial-resolution CCD camera. The polarizers and compensator are adjusted so that only light with polarization that has been altered by variations in the optical properties of the sample, such as carbon growth, passes through the final polarizer to the CCD. In this “null field” configuration the thickness of any deposited C on the sample is approximately proportional to the square-root of the light intensity recorded by the CCD allowing for the production of a “movie” of the process.¹² The NEIS has been demonstrated to have monolayer sensitivity. With prior knowledge of the optical constants at the 635 nm wavelength of the laser from *ex situ* spectroscopic ellipsometry (SE), one can, by measuring the ellipsometric angles Δ and Ψ directly, make an estimate of the actual thickness.

The capabilities of NEIS are demonstrated in Fig. 4. Figure 4(a) shows a NEIS image of the distribution of C on a witness plate after EUV exposure in the presence of resist outgassing. The time evolution of the normalized NEIS signal along a line through the center of the exposure spot is illustrated in Fig. 4(b). Figure 4(c) plots the normalized NEIS signal at the center of the spot as a function of exposure time. This is the first report of semiquantitative real-time imaging of the evolution of optics degradation during EUV exposure.

IV. PERFORMANCE

A. Witness sample resist-outgas exposures

Figure 5 shows *ex situ* characterization with spot-scanned SE and XPS of the contamination formed by exposing a

Ru-capped membrane light modulator witness plate to the outgas resulting from exposure of a resist-coated 200 mm wafer to a clearing dose of in-band EUV radiation. The nominal diameter of the SE beam was 300 μm and the angle of incidence was 70°. A Cauchy dielectric function ($1.695 + 0.0132/\lambda^2 + 0.0002/\lambda^4$; Ref. 13) was used to model the carbon deposit over the wavelength range (600–1670) nm. The nominal diameter of the XPS beam was 250 μm and the angle of incidence was 0°. The effective attenuation length based on experimental inelastic mean-free path measured by Lesiak *et al.* was used to calculate C thickness from photoelectron signal.¹⁴ Note that the thickness distribution reaches a plateau in the center rather than follow the quasi-Gaussian shape of the EUV intensity distribution found by both ray tracing and imaging of the EUV beam using a scintillator. This is an indication that the exposure was performed in the so-called “mass limited” regime, where the contamination rate is independent of intensity. This can be understood by considering that the contamination rate is proportional to the probability that a molecule adsorbed on the surface will undergo an EUV photon-induced reaction (either transformed chemically or desorbed by the photon or associated photoelectrons) before it leaves the surface by thermal desorption. This probability increases linearly with intensity until the photo-reaction rate becomes greater than the thermal desorption rate and the probability of photo-reacting before desorbing approaches unity. Increasing the intensity above this saturation value will not increase the contamination rate since every available molecule will already be consumed by photoreaction, hence the description as mass limited. It is an important requirement of resist-outgas-qualification tests that the intensity on the witness plate be greater than the saturation intensity. This ensures that the maximum amount of C is deposited for a given resist and that the ultimate qualification of the resist is not dependent on the accuracy of the intensity measurement.

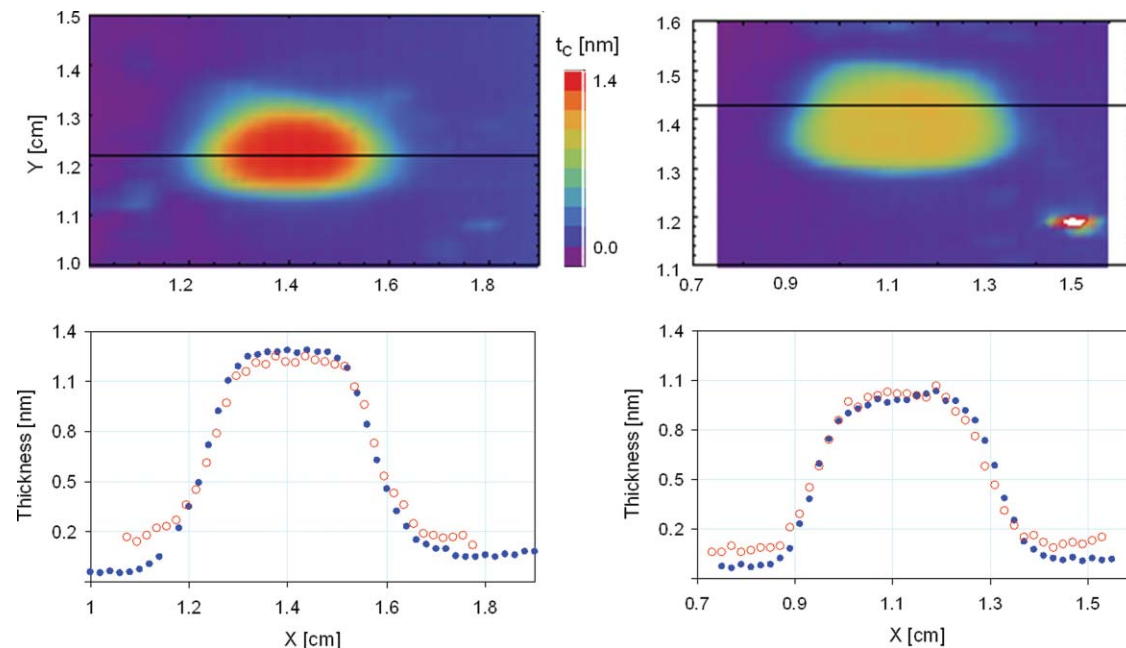


FIG. 5. (Color) Top: *ex situ* SE images of carbon deposits from two of the four tested resists. Color scale for both images is -0.2 nm to 1.4 nm . Bottom: SE (blue filled circles) and XPS (red open circles) line profiles of the carbon deposits.

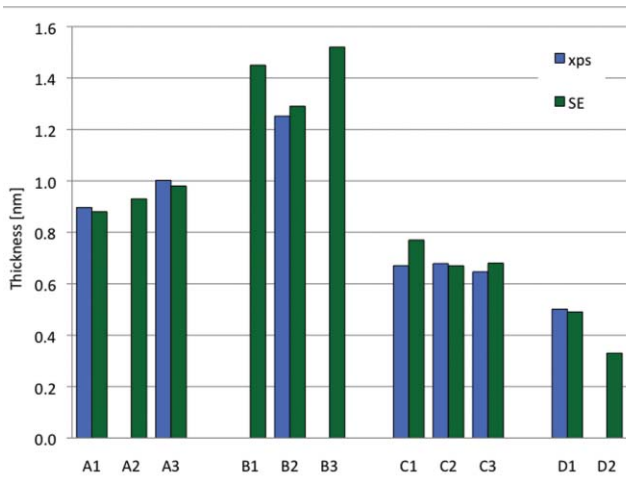


FIG. 6. (Color online) Carbon thickness in the exposure spots resulting from four different resists measured by XPS (light) and SE (dark).

Figure 6 shows the thicknesses of the flat-top area resulting from several repeated tests at the clearing dose for each of four different resists. These results demonstrate that the repeatability of our measurements is adequate for witness-plate testing. Moreover, our metrology is sensitive enough to clearly see the deposits even from the least-contaminating resist.

B. Dose-to-clear measurements

The facility can also be used for performing dose-to-clear, or E_0 measurements without changing any of the mechanical configuration. As mentioned, the scan speed of the rapidly rotating wafer across the exposure spot can be programmed to produce any dose desired, and that dose can be made a function of the radial position of the wafer. Figure 7 shows an example of such a measurement. To ensure an accurate result, we use the NIST-calibrated EUV-sensitive photodiode between the fold mirror and the wafer to measure the incident power as a function of synchrotron beam current, which remains linear to $\pm 1\%$. We then adjust the scan speed to compensate for the loss of beam current during an exposure and to obtain the desired dose for the radius. These tests are necessary, since the outgassing from a photoresist sample is related to the dose delivered. Such measurements can be useful on their own, since there has been some uncertainty in the past regarding measurement of dose-to-clear of EUV resists.¹⁵ For measurements such as these, our uncertainty (2σ) is 6%, which is dominated by a 5% uncertainty due to beam non-uniformity. Other contributions are from determining the position of the beam on the wafer (2%) and 1% contributions from detector calibration, linearity of synchrotron beam decay and mirror degradation, and our scanning algorithm. This compares favorably with our 15% uncertainty in E_0 measurements using a different apparatus.¹⁶ The uncertainty in that measurement was dominated by area and uniformity measurements of a very small spot, which are absent from the current measurements.

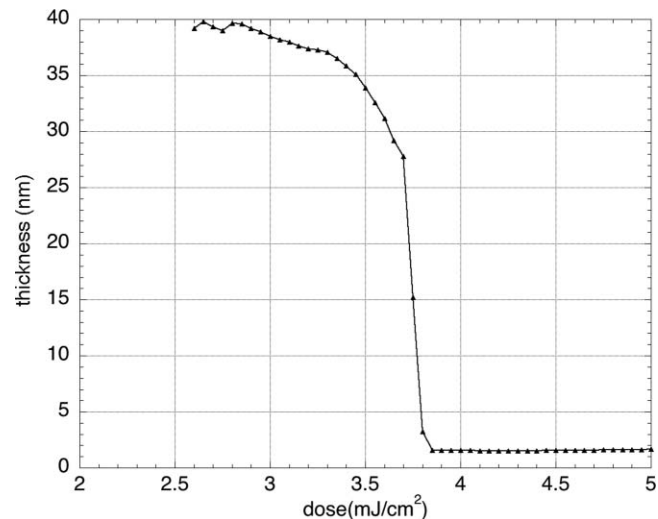


FIG. 7. Developed thickness of a sample photoresist as a function of dose, establishing the clearing-dose. The ≈ 1.7 nm offset after clearing is the native oxide of the substrate wafer.

V. SUMMARY

We have constructed a facility that allows for the exposure of an EUV optic in the presence of an outgassing resist in a configuration that simulates the conditions in a real scanner, but because of the absence of any mitigation provisions, provides for an accelerated test of contamination build-up. The facility is well suited not only for implementing the test protocol developed by toolmakers, but for providing benchmark measurements to set up equivalences with more accessible, in-field test facilities based on electron-beam irradiation and to serve as a test bed for developing more advanced testing protocols. The facility also provides for an accurate, rapid dose-to-clear measurements, and for the observation of real-time effects in contamination build-up through the *in situ* NEIS instrument.

ACKNOWLEDGMENTS

This work was supported in part by ASML. We would like to thank N. Harned and others at ASML for helpful conversations. Preparation of resist-coated substrates and ellipsometric mapping of developed resists was performed at the NIST Center for Nanoscale Science and Technology.

- ¹V. Bakshi, *EUV Lithography* (SPIE Press, Bellingham, WA, 2008).
- ²S. Bajt, N. V. Edwards, and T. E. Madey, *Surf. Sci. Rep.* **63**, 73 (2008).
- ³K. R. Dean, G. Denbeaux, A. Wuest, and R. Garg, *J. Photopolym. Sci. Technol.* **20**, 393 (2007).
- ⁴C. Tarrio and S. Grantham, *Rev. Sci. Instrum.* **76**, 056101–104 (2005).
- ⁵S. B. Hill, N. S. Faradzhev, C. Tarrio, T. B. Lucatorto, T. E. Madey, B. V. Yakshinskiy, E. Loginov, and S. Yulin, *Proc. SPIE* **6921**, 692117 (2008).
- ⁶N. Harned, http://ieuvi.org/TWG/Resist/2010/101710/Outgas-Testing_IEUVI-TWG_Noreen-Harned.pdf for information regarding witness plate testing methods and requirements.
- ⁷S. Bajt, H. N. Chapman, N. Nguyen, J. Alameda, J. C. Robinson, M. E. Malinowski, E. M. Gullikson, A. Aquila, C. Tarrio, and S. Grantham, *Appl. Opt.* **42**, 5750 (2003).
- ⁸U. Arp, A. P. Farrell, M. L. Furst, S. Grantham, E. Hagley, S. G. Kaplan, P.-S. Shaw, C. S. Tarrio, and R. E. Vest, *Synchrotron Radiat. News* **16**(5), 30 (2003).

- ⁹W. Thur, R. DeMarco, B. Baldock, and K. Rex, "Rigid, adjustable support of aligned elements via six struts" (unpublished).
- ¹⁰R. E. Vest and L. R. Canfield, *Synchrotron Radiation Instrumentation*, AIP Conference Proceedings Vol. 521, edited by P. Pianetta, J. Arthur, and S. Brennan, (AIP, Melville, NY, 2000), pp. 104–107.
- ¹¹R. Garg, N. S. Faradzhev, S. B. Hill, L. J. Richter, P.-S. Shaw, R. E. Vest, and T. B. Lucatorto, Proc SPIE **7636**, 76360E (2010).
- ¹²G. Jin, R. Jansson, and H. Arwin, Rev. Sci. Instrum. **67**, 2930 (1996).
- ¹³ASML, private communication (2010).
- ¹⁴B. Lesiak, A. Jablonski, Z. Prussak, and P. Mrozek, Surf. Sci. **223**, 213 (1989).
- ¹⁵P. P. Naulleau, E. M. Gullikson, A. Aquila, S. George, and D. Niakoula, Optics Express **16**, 11519 (2008).
- ¹⁶C. Tarrio, S. Grantham, M. Cangemi, R. E. Vest, T. B. Lucatorto, and N. Harned, Proc. SPIE **7271**, 72713x (2009).